

## REMOVAL OF ACID ORANGE II DYE BY GRANITIC NANO-ZERO VALENT IRON (nZVI) COMPOSITE

Nur 'Aishah Zarime<sup>1</sup>, Wan Zuhairi Wan Yaacob<sup>2</sup> and Habibah Jamil<sup>3</sup>

Geology Programme, Faculty of Science and Technology, Universiti Kebangsaan Malaysia, Malaysia

\*Corresponding Author: Received: 19 Nov. 2018, Revised: 29 Dec. 2018, Accepted: 10 Jan. 2019

**ABSTRACT:** The study highlights the effectiveness of nanoscale zero-valent iron (nZVI) composite in removing Acid Orange II dye. In this study, granitic residual soil has been used as supported material to stabilize the nanoscale zero-valent iron (nZVI) and to improve its adsorption capacity. The physical, chemical, mineralogical and morphological properties of the successfully synthesized granitic nano zero valent iron (Gr-nZVI) have been analyzed by Brunauer–Emmett–Teller (BET) surface area, X-ray Photoelectron Spectroscopy with Auger Electron Spectroscopy (XPS-AES), Field Emission Scanning Electron Microscopy (FESEM), and X-Ray Diffraction (XRD). The batch adsorption tests for the granitic residual soil (Gr) and the granitic nano-zero valent iron (Gr-nZVI) on Acid Orange II have been conducted to determine the effectiveness of both materials in dye removal. The five effects analyzed in the Batch test are concentration, dose, pH, kinetic and temperature. It was found that Gr-nZVI has higher absorption capacity compared to Gr. The effectiveness of Gr-nZVI composite in dye adsorption is due to the dispersion of nZVI particles on granitic soil particles, consequently providing more sites for adsorption. The results suggest that Gr-nZVI has potential as low-cost adsorbent for Acid Orange II removal from synthetic dye wastewater.

*Keywords: Granitic Residual Soil, Nano-Zero Valent Iron Composite, Batch Test, Acid Orange II*

### 1. INTRODUCTION

Huge amount of residual dyes from textile, tannery, paper, printing, paints, rubber and plastic industries are released to the environment and it would contaminate water and soil due to its toxicity and degradability [1-2]. Textile residual dye are highly resistant to light, pH and microbial attack render its existence in the environment for a longer period of time [3]. To overcome this environmental problem, material from nano zero valent iron (nZVI) are suggested to remove the residual dye. Recently, nZVI has been extensively studied for remediation and waste water treatment [4-7]. The nZVI are chosen due to its potential to decolorize azo-dyes rapidly without further treatments [8]. The nZVI also enhanced reactivity by increasing the surface area and volume ratios thus providing more reactive surface sites [4]. However, there are disadvantages of using nZVI because it has strong tendency to agglomerate into larger particles resulting in diminishing reactivity, and such condition in the treatment system are uneconomical due to the generation of secondary iron pollution [4]. To address this problem, composite nZVI has been proposed to stabilize the nZVI particles onto various supports. In this study, Gr-nZVI has been synthesized via chemical reduction method by using Ferric Chloride Tetrahydrate,  $\text{FeCl}_3 \cdot 6\text{H}_2\text{O}$  and Sodium Borohidrat,  $\text{NaBH}_4$ . The adsorption capacity of Gr-nZVI in by Batch test.

### 2. MATERIALS AND METHODS

#### 2.1 Materials

The granitic residual soil (BGR) from Broga, Selangor was used in this study. Acid Orange II was supplied in solid state with high purity (wt.% 99.9%) from Tianjin Yuhua Co., China. Chemical such as Ferric Chloride Tetrahydrate,  $\text{FeCl}_3 \cdot 6\text{H}_2\text{O}$  (Acros organics, 99 +%), Sodium Borohidrat,  $\text{NaBH}_4$  (Acros organics, 98 +%) and Ethanol  $\text{C}_2\text{H}_6\text{O}$  (Fisher Scientific, 99.4%) were used in this analysis.

#### 2.2 Synthesizing nZVI Composite

The granitic nano zero valent iron (Gr-nZVI) composite was synthesized by using chemical reduction method [9-10]. Ferric chloride solutions were prepared by mixing 4.38g ferric chloride tetrahydrate with 50 ml mixture of ethanol and deionized water (35ml ethanol + 15ml of deionized water). Granitic residual soil was added to ferric chloride solution and the mixture was shaken using ultrasonic shaker for 30 minutes. An amount of 6.091 g sodium borohydride were dissolved in 100 ml deionized water to produce  $\text{NaBH}_4$  solutions. The  $\text{NaBH}_4$  solutions were pipetted and were dropped (1 drop/ 2 seconds) into ferric chloride solution on a magnetic stirrer. The mixture was stirred for 20 minutes after the last dropped of  $\text{NaBH}_4$ . The black particles of Gr-nZVI composite

were filtered and were washed three times with ethanol (50ml). The Gr-nZVI composite was oven dried at 50°C for approximately 12 hours.

### 2.3 Characterization of nZVI Composite

The physical characterization of granitic residual soil, Gr and Gr-nZVI composite were analyzed using Brunauer–Emmett–Teller by N<sub>2</sub> desorption method to determine the specific area of particles. Chemical characterization was conducted by means of X-ray photoelectron spectroscopy and Auger Electron Spectroscopy (XPS-AES) to measure the surficial chemical composition and elements valence of particles. The morphology and mineralogy of the particles were characterized by Field Emission Scanning Electron Microscope (FESEM) and X-ray Diffraction (XRD). FESEM was performed by using Merlin Compact Supra 55VP where it was utilized the sound pulses transmitted through a particle suspension to determine the properties of the suspended particles [11]. Besides, XRD patterns for Gr and Gr-nZVI composite were also determined by Bruker/D8 Advance with a high-power Cu-K $\alpha$  radioactive source at 40kV/40mA.

### 2.4 Batch Test

The test was performed to study the removal of Acid Orange II using nanoparticles (nZVI) composite. Batch test method was reported by [12]. Gr and Gr-nZVI were prepared by passing the materials through 63 $\mu$ m sieve. Acid Orange II solution was prepared with 7 different concentrations, the 5 mg/L, 20 mg/L, 40 mg/L, 60 mg/L and 100 mg/L. To perform this test, 0.5 g of Gr-nZVI with 50 ml of Acid Orange II (1:100 ratio soil/solution) were mixed in centrifuge tubes. The mixture samples were shaken at 150 RPM for 3 hours to attain their equilibrium [13]. After shaking, mixture samples were centrifuged at 1500 RPM for 15 minutes and filtered through 45  $\mu$ m nitrocellulose membranes. The solutions were analyzed using UV-VIS Spectrophotometer (UV1201).

There are 5 effects in Batch test were analyzed including concentration, dose, pH, kinetic and temperature. To determine the optimum dosage, different dosage of materials (0.03 g, 0.05 g, 0.07 g, 0.1 g, 0.3 g, 0.5 g, 0.7 g, and 1.0 g) was used. The materials with different dose were added to 50ml Acid Orange II (50 mg/L). For pH effect, different pH of Acid Orange II (pH2, pH4, pH6, pH8, pH10 and pH12) was used. Kinetic effect represented by shaking time (5 min, 10 min, 20 min, 30 min, 45 min, 60 min, 120 min, 180 min and 360 min) while for temperature effect, different temperature (30 °C,

40 °C, 50 °C and 60 °C) was used in this analysis. For all factor, the batch test analysis was carried out with the ratio 1:100.

The concentration of Acid Orange II absorbed by particles,  $q_e$  was calculated using the formula as follows;

$$q_e = \frac{(C_o - C_e)V}{M} \quad (1)$$

Where;  $C_o$  and  $C_e$  representing initial concentration and equilibrium concentration respectively (mg/L),  $V$  is volume of solution added (ml),  $M$  is mass of air-dried material (g)

## 3. RESULTS AND DISCUSSIONS

### 3.1 Characterization of Nanoparticles (nZVI) Composite

Table 1 showed the result of specific surface areas (BET) for Granite residual soil (Gr) and granitic nZVI composite (Gr-nZVI). Gr showed higher surface area (14.1724 m<sup>2</sup>/g) compared to Gr-nZVI (6.7619 m<sup>2</sup>/g). Gr also showed higher pore volume (0.0484 cm<sup>3</sup>/g) compared to Gr-nZVI (0.0298 cm<sup>3</sup>/g). The results indicated that pores in the granitic residual soil were filled with added nZVI particles [14-15]. The larger surface area led to more uniform distribution of nZVI particles on the appropriate clay [16].

Table 1 Specific surface areas (BET) result for Granitic residual soil (Gr) and Granitic nZVI composite (Gr-nZVI)

Sampel	Gr	Gr-nZVI
BET Surface Area (m <sup>2</sup> /g)	14.1724	6.7619
Pore Volume (cm <sup>3</sup> /g)	0.0484	0.0298
Pore Size (Å)	136.6348 (13.66348 nm)	176.0732 (17.60732 nm)

Figure 1 and Figure 2 showed the X-ray photoelectron spectroscopy and Auger Electron Spectroscopy (XPS-AES) spectrum of Gr and Gr-nZVI. As displayed in Figure 1(a), Fe, O, C, Si and Al were found on the Gr surface while Na, Fe, O, C, B, Si and Al were distributed on Gr-nZVI surface. Na and B were expected to be present as NaBH<sub>4</sub> was used to synthesize Gr-nZVI [9]. To confirm the occurrence of Fe, the XPS-AES spectrum of the Fe 2p were displayed in Figure 1(b) and Figure 2(b). Figure 1(b) depicted the binding energy Fe 2p<sub>1/2</sub> 722.5 eV while for Gr-nZVI (Figure 2(b)) depicted binding energy of Fe 2p<sub>1/2</sub> 721.1 eV. Both peaks indicated the granitic surface as FeO. Granite

(igneous rock) composed of various minerals including quartz, potassium and plagioclase feldspars, crystalline iron-bearing minerals (commonly amphibole and magnetite), and micaceous minerals [17]. According to [9], the peaks at 719.7 eV (Fe0 2p<sub>1/2</sub>) corresponding to zero valent iron .

The morphologies of Gr and Gr-nZVI described by SEM and FESEM. Figure 3 shows the SEM image for Gr where it contained kaolinite, illite and halloysite minerals. Kaolinite was indicated by its well sheet shape while illite has unorganized sheet shape. Halloysite was identified by rod shape overlaid kaolinite minerals. These results were in agreement with report by [18]. Figure 4 shows FESEM image where the existence of nZVI can be

observed. The nZVI particles has spherical shapes and aggregated into a chain-like [19-20] on granitic soil surface. According to [21], aggregations of nZVI was due its huge interface energy and magnetic property. The nZVI particles size were in the ranged of 54.75 nm to 71.46 nm. The X-ray Diffraction (XRD) patterns for Gr and Gr-nZVI were presented in Figure 5. Gr in XRD pattern consisted of kaolinite, identified through peak of 2.55Å and 3.55Å. Illite was identified by the peak of 4.47Å and halloysite was identified by 3.62Å peak. Gr-nZVI showed that the kaolinite, illite and halloysite minerals were remained on the soil particles after synthesizing process. In Gr-nZVI, small peak at  $2\theta = 44.9^\circ$  corresponded to the formation of zero valent iron [7], [9].

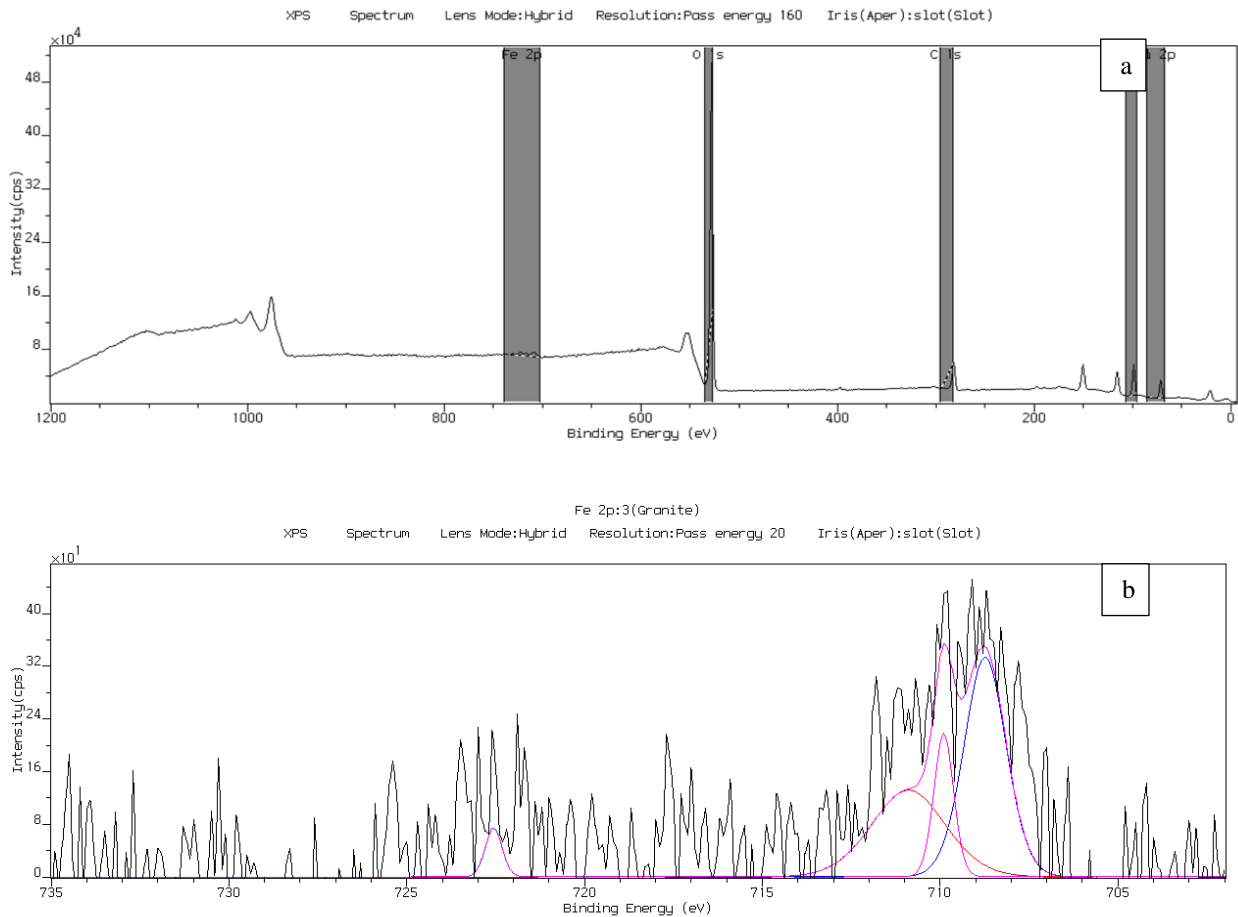


Fig.1 X-ray photoelectron spectroscopy and Auger Electron Spectroscopy (XPS-AES) result for granite, Gr (a) full Gr and (b) Fe 2p line

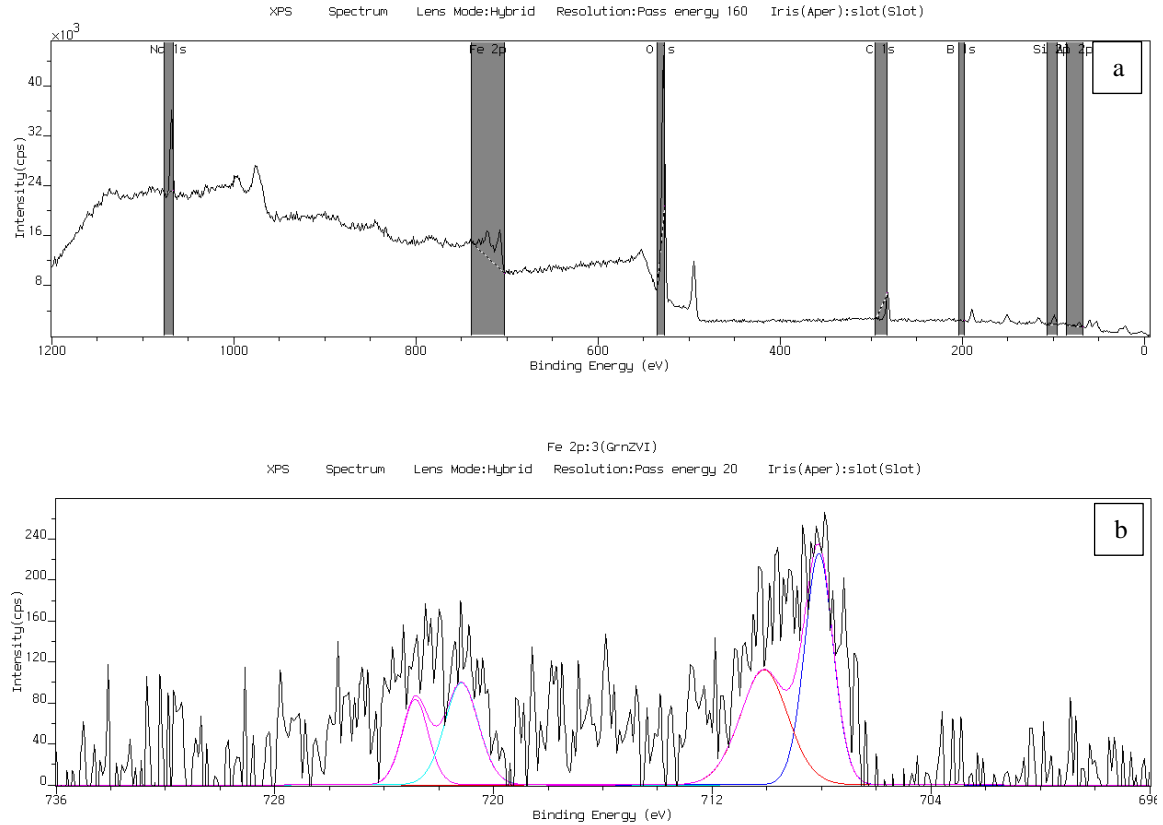


Fig.2 X-ray photoelectron spectroscopy with Auger Electron Spectroscopy (XPS-AES) result for Gr-nZVI, Gr (a) full Gr-nZVI and (b) Fe 2p line

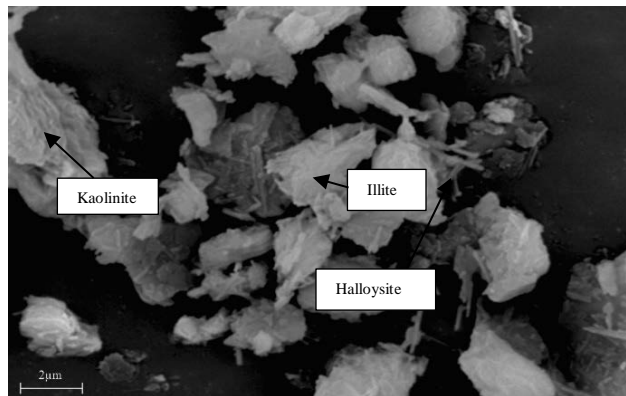


Fig.3 Scanning Electron Microscope (SEM) image with Mag=5000X for Gr sample.

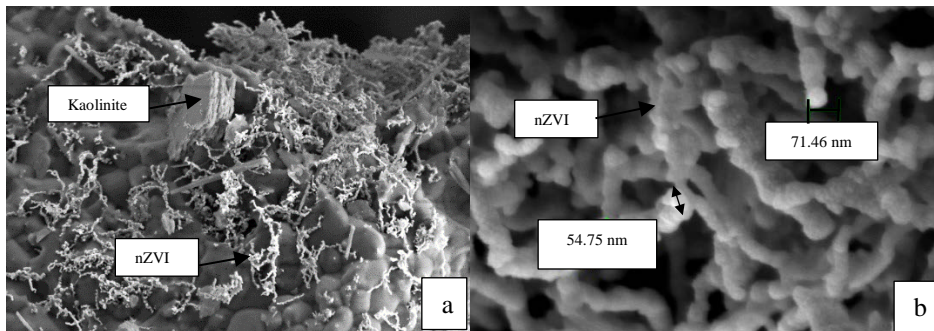


Fig.4 Field Emission Scanning Electron Microscope (FESEM) images for both Gr-nZVI (a) Mag=10000X and (b) Mag=100000X

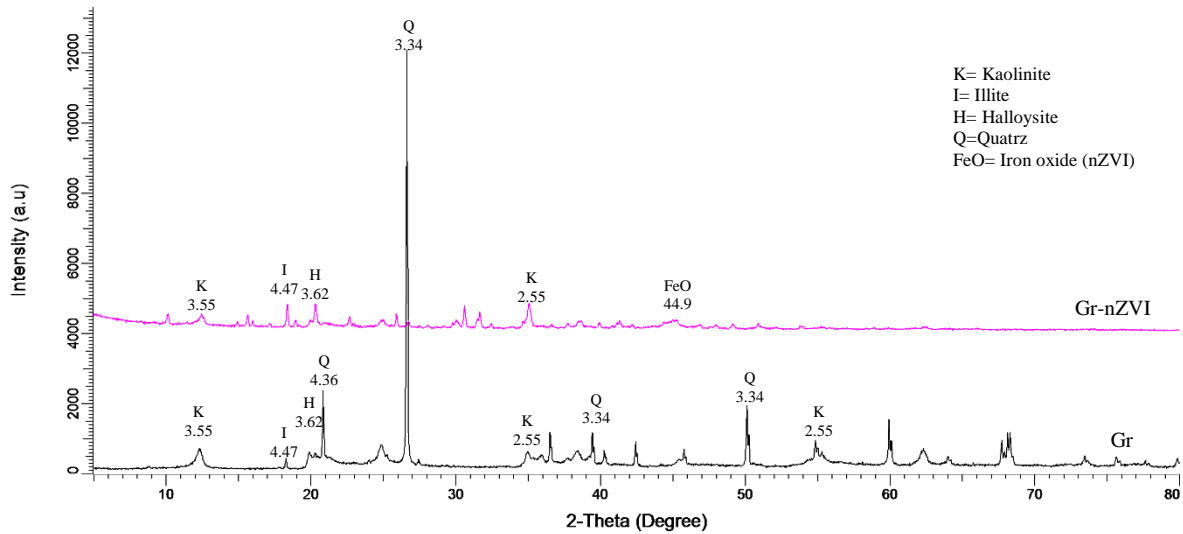


Fig.5 X-ray Diffraction (XRD) images for Gr and Gr-nZVI

### 3.2 Batch Test

Batch test was conducted to determine adsorption capacity of the materials (Gr and Gr-nZVI).

#### 3.2.1 Dose Effect

Figure 6 showed the adsorption of Acid Orange II by absorbent materials (Gr and Gr-nZVI) in different dosage. The results showed that, the adsorption capacity for both materials (Gr and Gr-nZVI) were decreased with the increase of adsorbent materials. According to [22], such condition was due to the overlapping of adsorption sites, rendering it overcrowded with adsorbent particles. The curve also depicted the Gr-nZVI adsorbed more dye than Gr. The equilibrium concentration after adsorption for Gr-nZVI and Gr was 5.3284 mg/g and 3.3800 mg/g respectively. According to [9, 23-24], higher adsorption capacity of Gr-nZVI was due to larger specific area and the availability of more adsorption sites to accelerate initial reaction. The optimum adsorbent dosages was 0.5 g and further experiments were carried out using this dose.

#### 3.2.2 Concentration Effect

The effect of initial concentration of Acid Orange II was investigated in the ranged of 5 mg/L to 100 mg/L and was presented in Figure 7. Based on its higher adsorption capacity, the Gr-nZVI proved as better adsorbent compared to Gr. The result also showed that the adsorption capacity increased with the increasing of initial concentration until at one point it became constant although the initial concentration was increased.

For Gr-nZVI, at initial concentration of 40 - 100 mg/L, the graph was constant, indicating the saturated Gr-nZVI surface no more dye or metal ions can be adsorbed [25]. The optimum metal concentration was determined as 40 mg/L.

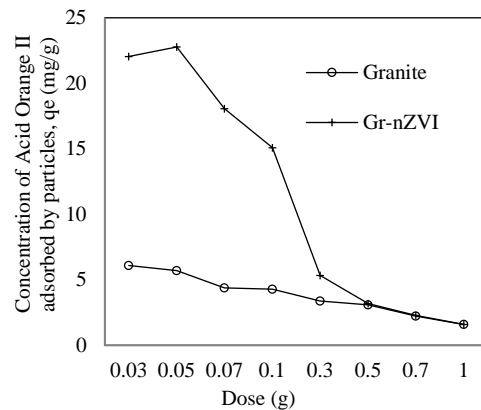


Fig.6 Effect of dosage in adsorption capacity of Gr and Gr-nZVI

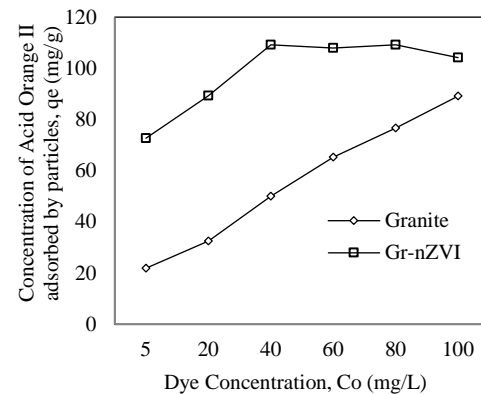


Fig.7 Effect of initial concentration of Acid Orange II in adsorption capacity of Gr and Gr-nZVI

### 3.2.3 pH Effect

The effect of pH on the adsorption of Acid Orange II by Gr and Gr-nZVI were shown in Figure 8 with initial dye concentration of 50 mg/L and adsorbent dosage 0.5g. From the graph, in all pH conditions, Gr-nZVI showed higher adsorption capacity ( $q_e$   $_{pH2}$  = 5.3284 mg/g) compared to Gr ( $q_e$   $_{pH2}$  = 3.0288 mg/g). The Gr-nZVI graph was constant suggesting that its adsorption capacity was not affected by pH values. However, according to [26], the maximum adsorption for DR23 and DR80 (anionic dye) was at pH 2. This was due to the strong electrostatic attraction between positively charged surface of the adsorbent and the anionic dye. As pH of dye increased, negative charged sites were also increased. Negative charged on the adsorbent's surface site did not favored the adsorption of ionic dye due to electrostatic repulsion. Gr curve showed the decreased of adsorption capacity with the increased of pH values. At higher pH, there was competition adsorption between OH<sup>-</sup> ions and anionic resulting lower adsorption capacity [26], [27].

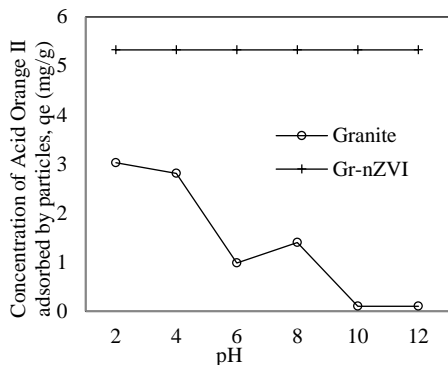


Fig.8 Effect of pH in adsorption capacity of Gr and Gr-nZVI

### 3.2.4 Kinetic Effect

Figure 9 shows the adsorption kinetics of Acid Orange II on Gr and Gr-nZVI. Both curves showed higher adsorption at the beginning and remained constant (reached equilibrium) after 5 minutes. A similar trend reported by [22]. According to [28], rapid phase was due to the presence of large number of vacant sites, which led to increase in concentration gradient between dye solution and adsorbent surface. The equilibrium time also depended on dye initial concentration. The lower dye initial concentration, the shorter the equilibrium time interval [28]. Gr-nZVI also showed better results in adsorbing Acid Orange II compared to Gr. Gr-nZVI provided both mineral and nZVI particle surfaces to adsorb dye. As reported by [4], the core shell of nZVI possessed hydroxyl groups when it

was interface with dye solution and it has their own capability to immobilize sorbate molecules by surface complexation. The nZVI core also formed an electron where it could reduce Acid Orange II.

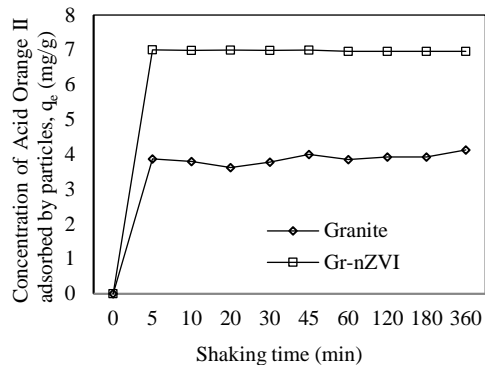


Fig.9 Effect of kinetic in adsorption capacity of Gr and Gr-nZVI

### 3.2.5 Temperature Effect

To understand the temperature effect of Acid Orange II on Gr and Gr-nZVI, the experiments were carried out at 30, 40, 50 and 60 °C with dye concentration of 50 mg/L and adsorbent dosage 0.5g. The results were displayed in Figure 10. Gr curve showed that dye adsorption capacity was increased with increasing of temperature. Similar results were reported by [23]. For Gr-nZVI, the curve was constant, and the adsorption capacity higher compared to Gr. The results showed that temperature effect did not give any significant effect on Gr-nZVI sample. Gr-nZVI provided both mineral and nZVI particles surfaces for greater adsorption sites compared to Gr. The findings suggesting the stability of Gr-nZVI towards temperature effects and proven as better materials for water treatment in the natural environment.

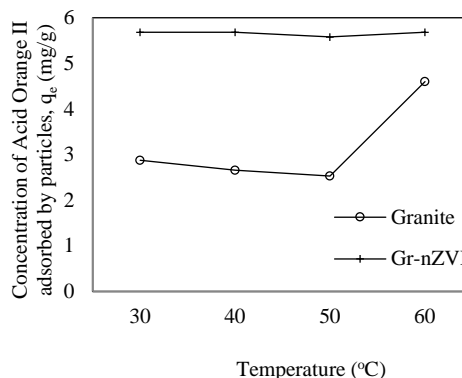


Fig.10 The effect of temperature in adsorption capacity of Gr and Gr-nZVI

#### 4. CONCLUSIONS

In this study, Gr-nZVI was proven as better materials in adsorbing Acid Orange II compared to Gr. Based on Batch test, Gr-nZVI was stable in all effects tested including concentration, dose, pH, kinetic and temperature effects. Since Gr was low-cost material and easily obtain, Gr-nZVI was chosen as remediation material to remove Acid Orange II and other anionic dyes in wastewater.

#### 5. ACKNOWLEDGEMENTS

This research project was supported by Centre for Research & Instrumentation Management (CRIM), UKM with financial support Ministry of Education. Authors acknowledged Geology Program, Faculty of Science and Technology, Universiti Kebangsaan Malaysia (UKM), Malaysia for their assistance in conducting this research.

#### 6. REFERENCES

- [1] Xi Y, Megharaj M., and Naidu R., Dispersion of zerovalent iron nanoparticles onto bentonites and use of these catalysts for orange II decolourisation. *Appl. Clay Sci.*, vol. 53, no. 4, 2011, pp. 716–722.
- [2] Zhang C., Zhu Z., Zhang H., and Hu Z., Rapid decolorization of Acid Orange II aqueous solution by amorphous zero-valent iron. *J. Environ. Sci.*, vol. 24, no. 6, 2012, pp. 1021–1026.
- [3] Selvanathan N., Subki N. S., and Sulaiman M. A., Dye Adsorbent by Activated Carbon. *J. Trop. Resour. Sustain. Sci.*, vol. 3, no. 1, 2015, pp. 169–173.
- [4] Luo S., Qin P., Shao J., Peng L., Zeng Q., and Gu J. D., Synthesis of reactive nanoscale zero valent iron using rectorite supports and its application for Orange II removal, *Chem. Eng. J.*, vol. 223, 2013, pp. 1–7.
- [5] Busch J., Meißner T., Potthoff A., Bleyl S., Georgi A., Mackenzie K., Trabitzsch R., Werban U., Oswald S.E., A field investigation on transport of carbon-supported nanoscale zero-valent iron (nZVI) in groundwater, *J. Contam. Hydrol.* Vol. 181, 2014.
- [6] Huang D., Chen G., Zeng G., Xu P., Yan M., Lai C., Zhang C., Li N., Cheng M., He X and He Y., Synthesis and Application of Modified Zero-Valent Iron Nanoparticles for Removal of Hexavalent Chromium from Wastewater, *Water, Air, Soil Pollut.*, vol. 226, no. 11, 2015, pp. 375.
- [7] Al-Dokheily M. E. and Sadoon A. A.-B. J., Synthesis of Iron Nanoparticles and Applications in the Removal of Heavy Metals from Aqueous Solutions, *Chem. Process Eng. Res.*, vol. 34, 2015.
- [8] Shih Y., Tso C., and Tung L., Rapid degradation of methyl orange with nanoscale zerovalent iron particles. *J. Environ. Eng. Manag.*, vol. 20, no. 3, 2010, pp. 137–143.
- [9] Yaacob W. Z. W. and How H. K., Synthesis and Characterization of Marine Clay-Supported Nano Zero Valent Iron, *Am. J. Environ. Sci.*, vol. 11, no. 2, 2015, pp. 115–124.
- [10] Rashmi S., Madhu G., Kittur A., and Suresh R., Synthesis, characterization and application of zero valent iron nanoparticles for the removal of toxic metal hexavalent chromium from aqueous solution. *Int. J. Curr. Eng. Technol.*, 2013, pp. 37–42.
- [11] Jamei M. R., Khosravi M., and Anvaripour B., Soil Remediation Using Nano Zero-valent Iron Synthesized by an Ultrasonic Method, *Iran. J. Oil Gas Sci. Technol.* vol. 1, no. 1, 2012, pp. 1–12.
- [12] USEPA, Batch-Type Procedures for Estimating Soil Adsorption of Chemicals, EPA/530/SW- 87/006-F, 1992.
- [13] Antoniadis V. and Tsadilas C. D., Sorption of cadmium, nickel, and zinc in mono- and multimetal systems, *Appl. Chem.*, vol. 22, 2007, pp. 2375–2380.
- [14] Zhu H., Jia Y., Wu X., and Wang H., Removal of arsenic from water by supported nano zero-valent iron on activated carbon, *J. Hazard. Mater.*, vol. 172, no. 2–3, 2009, pp. 1591–1596.
- [15] Chen Z. X., Cheng Y., Chen Z., Megharaj M., and Naidu R., Kaolin-supported nanoscale zero-valent iron for removing cationic dye-crystal violet in aqueous solution, *Nanotechnol. Sustain. Dev. First Ed.*, 2012 pp. 189–196.
- [16] Tomas'evic' D. D., Kozma G., Kerkez D. V., Dalmacija B. D., Dalmacija M. B., Bec'elic'-Tomin M. R., Kukovec A', Ko'nya Z., and Ronc'evic S., Toxic metal immobilization in contaminated sediment using bentonite- and kaolinite-supported nano zero-valent iron, *J. Nanoparticle Res.*, vol. 16, no. 8, 2014.
- [17] Jan Y., Wang T., Li M., Tsai S., Wei Y., and Teng S., Adsorption of Se species on crushed granite: A direct linkage with its internal iron-related minerals, *Applied Radiation and Isotopes.* vol. 66, 2008 pp. 14–23.
- [18] Robertson I. D. M., Weathering of Granitic Muscovite to Kaolinite and Halloysite and of Plagioclase-Derived Kaolinite to Halloysite, *Clays Clay Miner.* vol. 39, no. 2, 1991, pp. 113–126.
- [19] Shi L., Zhang X., and Liang Chen Z., Removal of Chromium (VI) from wastewater using bentonite-supported nanoscale zero-

- valent iron, *Water Res.* vol. 45, no. 2, 2011, pp. 886–892.
- [20] Kerkez D. V., Tomas̃evic' D. D., Kozma G., Bec̃elic'-Tomin M. R., Prica M. D., Ronc̃evic' S. D., Kukovecz A., Dalmacija B. D., and Ko' nya Z. Three different clay-supported nanoscale zero-valent iron materials for industrial azo dye degradation: A comparative study, *J. Taiwan Inst. Chem. Eng.*, vol. 45, no. 5, 2014, pp. 2451–2461.
- [21] Han L., Xue S., Zhao S., Yan J., Qian L., and Chen M., Biochar supported nanoscale iron particles for the efficient removal of methyl orange dye in aqueous solutions, *PLoS One*, vol. 10, no. 7, 2015, pp. 1–15.
- [22] Hefne J. A., Mekhemer W. K., Alandis N. M., Aldayel O. A., and Alajyan T., Removal of Silver ( I ) from Aqueous Solutions by Natural Bentonite, vol. 22, no. 1, 2010, pp. 155–176.
- [23] Reddy M. C. S., Sivaramakrishna L., and Reddy V., The use of an agricultural waste material, Jujuba seeds for the removal of anionic dye (Congo red) from aqueous medium., *J. Hazard. Mater.*, vol. 203–204, 2012, pp. 118–27.
- [24] Shu H. Y., Chang M. C., Chen C. C., and Chen P. E., Using resin supported nano zero-valent iron particles for decoloration of Acid Blue 113 azo dye solution, *J. Hazard. Mater.*, vol. 184, no. 1–3, 2010, pp. 499–505.
- [25] Veli S. and Alyüz B., Adsorption of copper and zinc from aqueous solutions by using natural clay., *J. Hazard. Mater.*, vol. 149, no. 1, 2007, pp. 226–33.
- [26] Arami M., Limaee N. Y., Mahmoodi N. M., and Tabrizi N. S., Removal of dyes from colored textile wastewater by orange peel adsorbent: Equilibrium and kinetic studies, *J. Colloid Interface Sci.*, vol. 288, no. 2, 2005, pp. 371–376.
- [27] Shen D., Fan J., Zhou W., Gao B., Yue Q., and Kang Q., Adsorption kinetics and isotherm of anionic dyes onto organo-bentonite from single and multisolute systems, *J. Hazard. Mater.* vol. 172, no. 1, 2009, pp. 99–107.
- [28] Babazadeh H., Nazemi, A. H. and Manshoury, M., Isotherm and Kinetic Studies on Adsorption of Pb, Zn and Cu by Kaolinite, *Caspian J. Env. Sci.*, vol. 9, no. 2, 2011, pp. 243–255.

---

Copyright © Int. J. of GEOMATE. All rights reserved, including the making of copies unless permission is obtained from the copyright proprietors.

---